HHS Public Access

Author manuscript

J Aerosol Sci. Author manuscript; available in PMC 2022 August 16.

Published in final edited form as:

J Aerosol Sci. 2021 June ; 155: . doi:10.1016/j.jaerosci.2021.105771.

Translating nanoparticle dosimetry from conventional *in vitro* systems to occupational inhalation exposures

Jordan Ned Smith[a,b,*], **Andrew W. Skinner**[a]

[a]Biological Sciences Division, Pacific Northwest National Laboratory (PNNL), Richland, WA, 99354, USA

[b]Department of Environmental and Molecular Toxicology, Oregon State University, Corvallis, OR 97331, USA

Abstract

As encouraged by *Toxicity Testing in the 21*st *Century*, researchers increasingly apply high-throughput *in vitro* approaches to identify and characterize nanoparticle hazards, including conventional aqueous cell culture systems to assess respiratory hazards. Translating nanoparticle dose from conventional toxicity testing systems to relevant human exposures remains a major challenge for assessing occupational risk of nanoparticle exposures. Here, we explored existing computational tools and data available to translate nanoparticle dose metrics from cellular test systems to inhalation exposures of silver nanoparticles in humans. We used the Multiple-Path Particle Dosimetry (MPPD) Model to predict nanoparticle deposition of humans exposed to 20 and 110 nm silver nanoparticles at 0.9 μg/m^3 over an 8 h period, the proposed National Institute of Occupational Safety and Health (NIOSH) recommended exposure limit (REL). MPPD predicts 8.1 and 3.7 μg of silver deposited in an 8 h period for 20 and 110 nm nanoparticles, respectively, with 20 nm particles displaying nearly 11-fold higher total surface area deposited. Peak deposited nanoparticle concentrations occurred more proximal in the pulmonary tract compared to mass deposition patterns (generation 4 vs. generations 20–21, respectively) due to regional differences in lung lining fluid volumes. Assuming 0.4% nanoparticle dissolution by mass measured in previous studies predicted peak concentrations of silver ions in cells of 1.06 and 0.89 μg/mL for 20 and 110 nm particles, respectively. Both predicted concentrations are below the measured toxic threshold of 1.7 μg/mL of silver ions in cells from *in vitro* assessments. Assuming 4% dissolution by mass predicted 10-fold higher silver concentrations in tissues, peaking at 10.6 and 8.9 μg/mL, for 20 and 110 nm nanoparticles respectively, exceeding the observed *in vitro* toxic threshold and highlighting the importance and sensitivity of dissolution rates. Overall, this approach offers a framework for extrapolating nanotoxicity results from *in vitro* cell culture systems to human exposures. Aligning appropriate dose metrics from *in vitro* and *in vivo* hazard characterizations and human pulmonary doses from occupational exposures are critical components for successful nanoparticle risk assessment and worker protection providing guidance for designing future *in vitro* studies aimed at relevant human exposures.

[*]Corresponding author. PO Box 999, Richland, WA, 99352, USA. jordan.smith@pnnl.gov (J.N. Smith).

Declaration of competing interest

The authors declare that they have no known competing financial interests or personal relationships that could have appeared to influence the work reported in this paper.

Keywords

I*n vitro* to *in vivo* extrapolation; Nanoparticle; Dosimetry modeling; Dose metrics

1. Introduction

Nanotechnology continues to rapidly expand and enhance consumer products worldwide. Found in nearly half of consumer products registered in nano-product databases, silver nanomaterials are among the most frequently utilized in consumer products (Nowack et al., 2011; Reidy et al., 2013; Weldon et al., 2016). Antimicrobial colloidal silver products were first registered for use in the United States during the 1950s (Nowack et al., 2011; Reidy et al., 2013). More recently, the number of products that use silver nanomaterials and volume of product use sharply increased. In 2010, manufacturers produced >400 different products containing an estimated 20 tons of silver nanomaterials in the United States (Hendren et al., 2011; Weldon et al., 2016). Highest exposures to silver nanomaterials are expected to occur to workers manufacturing or incorporating silver nanomaterials into consumer products such as textiles or electronics (Weldon et al., 2016). Reported occupational exposures range from 0.02 to 1.35 $\mu g/m^3$ in the air of silver nanomaterial production facilities (Lee et al., 2011; Weldon et al., 2016).

As encouraged by *Toxicity Testing in the 21*st *Century*, toxicologists increasingly apply high-throughput *in vitro* approaches to identify and characterize nanomaterial hazards in an effort to maintain pace with nanomaterial development and utilization (Fröhlich, 2018; Kumar et al., 2017; Nel et al., 2013; Paur et al., 2011; Savage et al., 2019). Researchers utilize high throughput cellular testing models including submerged cells, 2D and 3D cell cultures, air-liquid-interface systems, and other elaborate systems to expose cells to nanoparticles and evaluate potential perturbations to lung physiology. Using these systems, researchers have observed inflammatory responses, oxidative stress, and cytotoxicity in cultured cells exposed to silver nanoparticles (Johnston et al., 2010).

Toxicologists have recently gained a better appreciation for the complexities of nanomaterial dosimetry in these testing systems. Unique properties of nanomaterials (e.g. size, shape, density, agglomeration state, etc.) determine particle transport, dissolution, and intracellular fate, which all contribute to the delivered *in vitro* cellular dose (DeLoid et al., 2014; Hinderliter et al., 2010; Schmid & Cassee, 2017; Sharma et al., 2014; Teeguarden et al., 2007, 2014). Our group developed computational models to predict nanoparticle diffusion, sedimentation, and dissolution in conventional submerged cell culture systems (Hinderliter et al., 2010; Thomas et al., 2018). Hinderliter et al. developed the *in vitro* sedimentation, diffusion, and target cell dosimetry (ISDD) model to predict the cell-associated dose fraction of nanoparticles administered to cells during *in vitro* toxicity studies (Hinderliter et al., 2010). ISDD accounts for the deposition of particles onto the cells due to particle sedimentation and diffusion in liquid medium above the cells.

Under standard cell culture conditions, silver nanoparticles agglomerate and dissolve (Liu et al., 2010, 2012; Liu & Hurt, 2010; Munusamy et al., 2015), exposing cells to a complex mixture of nanoparticles, ions, and ion-ligand complexes with cell culture

medium constituents. This complex exposure has created uncertainty regarding the extent to which each constituent—ion, ion-protein complex, particle—contributes to observed cellular toxicity (Beer et al., 2012; Johnston et al., 2010; Reidy et al., 2013). ISDD is unable to predict dosimetry of soluble or semi-soluble nanoparticles (e.g. silver) since reduction in particle size impacts particle transport.

To address this shortfall, Thomas et al. developed a computational model (ISD3) to predict silver particle and ion dosimetry in conventional submerged cellular toxicity testing models (Thomas et al., 2018). Smith et al. applied ISD3 to silver nanoparticle toxicity studies to better understand the dosimetry of silver nanoparticle toxicity. (Smith et al. (2018)) observed loss of cellular viability in three types of macrophages (RAW 264.7 macrophages and bone marrow derived macrophages from wild-type C57BL/6J mice and Scavenger Receptor A deficient mice) after exposure to two diameters of silver nanoparticles (20 or 110 nm) or silver ions only at varying exposure levels (Smith et al., 2018). Smith et al. applied dose-response modeling to dose metrics predicted by ISD3 and identified silver ion levels in cells formed from extracellular nanoparticle dissolution as the best predictor of observed toxicity (Smith et al., 2018). A consistent threshold of 1.7 μg/mL silver ion concentration in cells resulted in 20% loss of viability (LD_{20}) across cell type, silver nanoparticle exposure, and silver ion exposures (Smith et al., 2018). But, what does this mean in the context of human inhalation exposures?

Translating nanoparticle dose from conventional toxicity test systems to human exposures remains a major challenge for assessing occupational risk of nanoparticles. Here, we explored existing computational tools and data available to translate this identified dose metric from cell tests systems to humans. We used the Multiple-Path Particle Dosimetry (MPPD) Model (Anjilvel & Asgharian, 1995; Miller et al., 2016) to predict deposition of occupationally relevant silver nanoparticle inhalation exposures and literature data sets to predict resulting nanoparticle concentrations and extent of dissolution. We utilized measured silver ion partitioning coefficients to predict silver ion concentrations in pulmonary tissues (Thomas et al., 2018) and compared silver ion concentrations in tissues to the *in vitro* toxic threshold in macrophages (Smith et al., 2018). Finally, we identified areas for further development to translate nanoparticle dose from cell systems to inhalation exposures more broadly across additional particles for nanoparticle risk assessment.

2. Materials and Methods

2.1. Nanoparticle deposition

We used MPPD (v3.04) to predict silver nanoparticle deposition throughout the pulmonary tract (Anjilvel & Asgharian, 1995; Miller et al., 2016). MPPD is a mechanistic particle dosimetry model that calculates regional and site-specific deposition and clearance of particles in the pulmonary tract of several species, including humans, rats, and mice. We used MPPD to simulate a 1-day occupational exposure to silver nanomaterials. For occupational exposures, National Institute of Occupational Safety and Health (NIOSH) has proposed a recommended exposure limit (REL) for silver nanoparticles of 0.9 $\mu g/m^3$ (NIOSH, 2018). A NIOSH REL is defined as a concentration of a potential hazard in the workplace air to protect worker health. NIOSH identified lung inflammation and function

deficits and liver bile duct hyperplasia as relevant adverse effects for which the silver nanoparticle REL is indented to protect against (NIOSH, 2018). While RELs are generally considered protective over a working lifetime of exposure, RELs are also relevant over shorter timeframes, such as a working day, and are expressed as 8 h time-weighted averages (TWA). As such, we simulated constant exposure of 0.9 $\mu g/m^3$ to 20 or 110 nm silver nanoparticles for 8 h (Table 1). We assumed the nanoparticles did not agglomerate, were inhaled as primary particles, and the nanoparticle density was 10.49 g/cm^3, the same as the bulk silver. The Pacific Northwest National Laboratory (PNNL) symmetrical lung geometry was utilized, which was derived from imaging the pulmonary tract of a human male of 35 years of age and 68 kg body weight (Kabilan et al., 2016). MPPD default values for various pulmonary physiological parameters of the PNNL symmetrical lung geometry were utilized (Table 2). Oronasal-normal augmenter breathing and respiratory parameters for light work were used to simulate occupational exposures (Table 2) (ICRP, 2002). We also assumed no particle clearance in order to simplify simulations. We acknowledge that this assumption will overestimate particle loads in the pulmonary tract. Similarly, in previous nose-only inhalation or intratracheal installation studies with silver nanoparticles studies, scientists observed that MPPD modestly overpredicts silver levels in pulmonary tracts of rats due to not accounting for nanoparticle dissolution, silver lung clearance (nanoparticles or ions), or other ventilation changes that occur during silver nanoparticle exposures (Braakhuis et al., 2014; Kreyling et al., 2020; Park et al., 2019). Accurate longer timescale occupational simulations require accurate estimates of silver particulate systemic absorption and clearance in humans as well as disposition of silver ions following nanoparticle dissolution.

2.2. Lung lining fluid volume

Lung lining fluid is a heterogenous thin layer of fluid that lines the pulmonary tract consisting of water, proteins, surfactants, glycoproteins, lipids, and salts (Ng et al., 2004). Lung lining fluid offers lubrication and protection to the pulmonary tissues and maintains a pH of ~6.9 (Ng et al., 2004). We used the volume of lung lining fluid to calculate deposited nanoparticle concentrations. We estimated lung lining fluid volume using MPPD reported surface area of the human lung and measured depths of lung lining fluid at different regions of the lung (Wauthoz & Amighi, 2015) (Table 3). Although lung lining fluid is known to be continuously secreted and have low levels of flow (Grotber, 2011), we assumed lung lining fluid volume and flow was static for these simulations.

2.3. Nanoparticle dissolution

Several studies investigated silver nanoparticle dissolution in various surrogates of lung lining fluid (Leo et al., 2013; Maurer et al., 2014; Stebounova et al., 2011; Sweeney et al., 2016). In order to mimic lung lining fluid, these studies used buffer solutions (7 pH) and coated the nanoparticles with surfactants found in lung lining fluid, either dipalmitoylphosphatidylcholine (DPPC), the most common phospholipid pulmonary surfactant, or Curosurf®, a natural pulmonary surfactant prepared from porcine lungs (Botelho et al., 2016; Leo et al., 2013; Stebounova et al., 2011; Sweeney et al., 2016). These studies observed low levels of silver nanoparticle dissolution (~0.4% by mass) when using pulmonary surfactants, and we used this factor to calculate nanoparticle dissolution in the pulmonary tract (Leo et al., 2013; Sweeney et al., 2016). Additional factors that

affect nanoparticle dissolution, like ranges of nanoparticle concentrations (we predict ≤2.5 μg/mL nanoparticle concentration (see Results) compared to previously tested nanoparticle concentration of 25 μg/mL) with multiple particle diameters (prior studies tested 20 nm only), have not been robustly evaluated in lung lining fluids (Leo et al., 2013; Sweeney et al., 2016). As such, we included 4% nanoparticle dissolution by mass to capture the possibility of higher dissolution amounts.

2.4. Ion partitioning

Previously, Thomas et al. developed a cellular uptake model for silver ions to simulate cellular levels of silver ions formed from extracellular nanoparticle dissolution (Thomas et al., 2018). This model assumes diffusion transport of silver ions and was modeled using a diffusion-limited uptake equation defined by Fick's Law of Diffusion. The model was parameterized by measuring cellular uptake of silver ions over time at 0.5 or 1.5 μg/mL silver ion concentration in cell culture media (Thomas et al., 2018). Thomas et al. observed steady-state silver partitioning in ~1 h at proportional concentrations of silver ion in cells and media (Thomas et al., 2018). Using this data, Thomas et al. calculated a cell:media silver ion partitioning coefficient of 25.8 (Thomas et al., 2018). Here, we used this partitioning coefficient to calculate silver ion concentrations in pulmonary tissues following nanoparticle inhalation, deposition in the pulmonary tract, and regional dissolution.

3. Results

After simulating occupational human inhalation exposures to both 20 and 110 nm silver nanoparticles, MPPD predicted diameter-dependent patterns of deposition. Using assumptions outlined in the Materials and Methods, MPPD predicted 2-fold higher levels of total fractional deposition (generations 1 to 24) for 20 nm nanoparticles compared to 110 nm nanoparticles (0.72 vs. 0.33, respectively). While a higher fraction of 20 nm particles deposited in the pulmonary tract compared to 110 nm particles, patterns of deposition as a function of pulmonary generation number were similar between the two particle diameters. Peak fractional deposition occurred at generation 20 for 20 nm particles, and similarly, 110 nm particles peaked at generation 21 (Fig. 1A). After exposure to the proposed NIOSH REL for silver nanoparticles (0.9 $\mu g/m^3$), MPPD predicts 8.1 and 3.7 μg of silver deposited in an 8 h period for 20 and 110 nm nanoparticles, respectively (Fig. 1B). Deposition of 20 nm nanoparticles exceed 110 nm nanoparticles by nearly 11-fold as a function of total surface area deposited (2.31 vs 0.21 cm^2, respectively) (Fig. 2).

We predict 1.2-fold higher peak concentrations of 20 nm silver nanoparticles compared to 110 nm nanoparticles using MPPD to predict nanoparticle deposition and estimating volumes of lung lining fluid (10.2 vs. 8.7 vs μg/mL, respectively) (Fig. 3). While overall nanoparticle concentration deposition patterns were similar between the particles, nanoparticle concentrations were 5–300% higher for 20 nm nanoparticles compared to 110 nm nanoparticles, except for the last generation. Peak nanoparticle concentrations occurred more proximal in the pulmonary tract compared to mass deposition patterns (Fig. 3 vs. Fig. 1B). Peak levels of nanoparticle concentration occurred at generation 4 for both 20 and 110 nm particles (Fig. 3), while peak mass was deposited at generations 20 and 21 (Fig.

1B). This observation highlights the importance of lung lining fluid volumes in the context of potential toxicity mediated by extracellular nanoparticle dissolution, since researchers have observed both rate of dissolution and extent of dissolution depend on nanoparticle concentrations (Munusamy et al., 2015).

Using a constant fraction of mass to estimate extent of nanoparticle dissolution, estimated concentrations of silver ions in cells followed similar patterns as concentrations of silver nanoparticles. Peak concentrations of silver ions in cells occurred at generation 4 for both 20 and 110 nm nanoparticles (Fig. 4). Assuming 0.4% dissolution by mass as previously measured with 20 nm silver nanoparticles in artificial lung lining fluid (Leo et al., 2013; Sweeney et al., 2016) predicted peak concentrations of silver ions in cells of 1.06 and 0.89 μg/mL for 20 and 110 nm particles, respectively (Fig. 4A). Both predicted concentrations are below the observed toxic threshold of 1.7 μg/mL of silver ions in cells (Smith et al., 2018). Assuming 4% dissolution by mass predicted 10-fold higher silver concentrations in tissues, peaking at 10.6 and 8.9 μg/mL (Fig. 4B). Under this assumption, 20 nm exposures would exceed the toxic threshold of 1.7 μg/mL of silver ions in cells at generations 2–13 as would 110 nm exposures at generations 2–9 (Fig. 4B).

4. Discussion

The purpose of this study was to explore existing computational tools and data available to translate dose metrics from cell systems to humans for nanoparticle exposures. We used MPPD coupled with existing lung lining fluid and nanoparticle dissolution data to predict regional dose metrics of nanoparticle exposures. We compared these dose metrics to threshold toxicity values identified using *in vitro* systems.

Overall, these results demonstrate that extent of silver nanoparticle dissolution is a critical and sensitive factor in determining silver nanoparticle toxicity from extracellular nanoparticle dissolution. Using the best available dissolution measurements with lung lining fluid surrogates (Leo et al., 2013; Sweeney et al., 2016), this model predicts that exposures to the proposed NIOSH REL for silver nanoparticle exposures should not exceed toxic threshold of silver ions measured in cells during an 8 h shift. However, if nanoparticle dissolution is higher (≥1% for 20 nm nanoparticles), we would expect silver ion concentrations to exceed the toxic threshold observed with *in vitro* assays (Smith et al., 2018).

We identified a handful of studies that evaluated silver nanoparticle dissolution in various surrogates of lung lining fluid (Leo et al., 2013; Maurer et al., 2014; Stebounova et al., 2011; Sweeney et al., 2016). In order to mimic lung lining fluid, these studies used buffer solutions (7 pH) and coated the nanoparticles with surfactants found in lung lining fluid, either DPPC, the most common phospholipid pulmonary surfactant, or Curosurf®, a natural pulmonary surfactant prepared from porcine lungs (Botelho et al., 2016; Leo et al., 2013; Stebounova et al., 2011; Sweeney et al., 2016). In general, lung lining surfactants attenuated silver nanoparticle dissolution compared to uncoated nanoparticles. Using 25 μg/mL of 20 nm silver nanoparticles, Leo et al. observed that DPPC (100 mg/L) delayed dissolution compared to no DPPC controls and observed very low levels of dissolution

at pH 7 (~0.5%) (Leo et al., 2013). Also using 25 μg/mL of 20 nm silver nanoparticles, Sweeney et al. observed ~0.4% dissolution with 1:1000 dilution of Curosurf® (Sweeney et al., 2016). Both of these studies observed lower levels of dissolution compared to other studies measuring dissolution of silver nanoparticles coated with fetal bovine serum in cell culture media (3–50% depending on particle diameter and concentration) (Botelho et al., 2016; Leo et al., 2013; Munusamy et al., 2015; Sweeney et al., 2016). These observations suggest a discrepancy between pulmonary and cell culture exposures: low dissolution in lung lining fluid and high dissolution in cell culture medium. Since silver nanoparticle dissolution is a key predictor of toxicity (Smith et al., 2018), this suggests that cell culture experiments may be more vulnerable to nanoparticle toxicity than pulmonary exposures. Furthermore, potential differences of dissolution rates between model test conditions and *in vivo* conditions highlights the importance of translating appropriate dose metrics between systems for meaningful comparisons.

Nanoparticle dissolution rates depend on nanoparticle concentration, nanoparticle size, various other constituents within the liquid medium, and their respective concentrations as well as temporal considerations (Munusamy et al., 2015). Here, we predict ≤2.5 μg/mL silver nanoparticle regional concentrations throughout the pulmonary tract following nanoparticle exposures (Fig. 3), ≥10-fold lower than concentrations used to measure nanoparticle dissolution in lung lining fluid surrogates (Leo et al., 2013; Sweeney et al., 2016). Munusamy et al. observed higher factions of dissolution at lower nanoparticle concentrations in cell culture media (Munusamy et al., 2015), suggesting that 0.4% dissolution could be a low estimate. As such, additional concentrations of silver nanoparticles may need to be evaluated to ensure the extent of nanoparticle dissolution does not exceed levels expected to cause toxicity. While 110 nm silver nanoparticles dissolve slower and to a lesser extent than 20 nm particles on an equal concentration basis (Munusamy et al., 2015; Thomas et al., 2018), additional experiments in lung lining fluid surrogates may be useful, especially if kinetic models of nanoparticle dissolution are needed.

Lung lining fluid volume was identified as another important factor with a moderate level of uncertainty. Fröhlich et al. published a review of reported lung lining fluid volumes and noted that measuring or estimating lung lining fluid was not straight forward and was somewhat difficult (Fröhlich et al., 2016). Consequently, overall estimates of lung lining fluid volumes are variable without robust consensus (Fröhlich et al., 2016). In this paper, we estimated lung lining fluid volume using the pulmonary tract surface area with reported depths of lung lining fluid at various regions (Wauthoz & Amighi, 2015). This approach estimated a total volume of lung lining fluid of 30 mL, which is consistent with other estimates which range 10–70 mL in humans (Fröhlich et al., 2016). Our estimate approximates lung lining fluid volumes extrapolated to humans (26 mL) from measurements in sheep using ^{125}I-albumin, a reliable measurement method that is difficult to conduct in live humans (Stephens et al., 1996).

Three major limitations of our approach should be addressed in future nanoparticle modeling efforts: modeling kinetics, clearance, and validation. Existing tools and/or data did not allow us to calculate the kinetics of nanoparticle deposition, clearance, and dissolution, without significant model development and resource commitment. The kinetics of clearance

and dissolution will significantly impact nanoparticle residence time after deposition. In short-term exposures, as we have conducted here, nanoparticle residence time is probably of little consequence. However, when considering long-term chronic exposures over work weeks or even lifetime exposures, if nanoparticle residence time is sufficiently long, bioaccumulation of nanoparticles could lead to scenarios in which toxicity thresholds could be achieved. In rodent models, reported half-lives of total silver (i.e. particles and ions) range from 2 to 4 d in early phases to 60–100 d in later phases following nanoparticle inhalation exposures (Anderson et al., 2015; Jo et al., 2020). These half-lives are a function of nanoparticle dissolution, mucociliary clearance, translocation to systemic circulation, and silver ion kinetics. Refinement of all these rates in humans may be necessary for further model development. Additionally, nanoparticle dissolution kinetics may impact total ion concentrations and determine “fresh” unbound ion concentrations. Silver ions bind to various ligands, and Smith et al. observed that “fresh” or unbound silver ions were toxic to macrophages while “aged” or bound silver ions were not toxic (Smith et al., 2018). Similarly, Kreyling et al. observed rapid dissolution of silver nanoparticles, formation of a salt layer around nanoparticles slowing dissolution, and precipitation of low soluble silver ions salts *in vivo* (Kreyling et al., 2020). This observation along with the *in vitro* work suggests that extent of nanoparticle dissolution soon after deposition may be a critical determinant in toxicity associated with inhaled silver nanoparticles. As such, future efforts should focus on refining relevant parameters for kinetics of nanoparticle clearance and dissolution in humans. Finally, model validation is required in order to for this model to meet regulatory requirements for human risk assessment of nanoparticles or set occupational workplace exposure limits.

Overall, the approach presented here offers a framework for extrapolating nanotoxicity results from *in vitro* systems to human exposures. We demonstrated how this approach can translate previously identified dose metrics from *in vitro* studies to human occupational exposures. Aligning appropriate dose metrics from *in vitro* hazard characterizations to *in vivo* human pulmonary doses from occupational exposures are critical components for successful nanoparticle risk assessment and worker protection. Additionally, this approach can provide exposure guidance for designing future *in vitro* studies aimed at relevant human exposures. Accurate *in vitro* to *in vivo* translations are paramount for realizing the vision of *Toxicity Testing in the 21*st *Century* and safely maximizing the potential of nanotechnology.

Acknowledgements

This publication was supported by funding from Centers for Disease Control and Prevention/National Institute for Occupational Safety and Health, CDC/NIOSH) grant R01 OH011023. Findings in this study were those of the authors, and do not necessarily reflect the official opinion of CDC/NIOSH. Authors give thanks to FN Smith and KA Gaither for thoughtful revision suggestions.

References

Anderson DS, Patchin ES, Silva RM, Uyeminami DL, Sharmah A, Guo T, & Van Winkle LS (2015). Influence of particle size on persistence and clearance of aerosolized silver nanoparticles in the rat lung. Toxicological Sciences, 144(2), 366–381. 10.1093/toxsci/kfv005 [PubMed: 25577195]

Anjilvel S, & Asgharian B (1995). A multiple-path model of particle deposition in the rat lung. Fundamental and Applied Toxicology, 28(1), 41–50. 10.1006/faat.1995.1144 [PubMed: 8566482]

Beer C, Foldbjerg R, Hayashi Y, Sutherland DS, & Autrup H (2012). Toxicity of silver nanoparticles - nanoparticle or silver ion? Toxicology Letters, 208(3), 286–292. 10.1016/j.toxlet.2011.11.002 [PubMed: 22101214]

Botelho DJ, Leo BF, Massa CB, Sarkar S, Tetley TD, Chung KF, & Gow AJ (2016). Low-dose AgNPs reduce lung mechanical function and innate immune defense in the absence of cellular toxicity. Nanotoxicology, 10(1), 118–127. 10.3109/17435390.2015.1038330 [PubMed: 26152688]

Braakhuis HM, Gosens I, Krystek P, Boere JA, Cassee FR, Fokkens PH, & Park MV (2014). Particle size dependent deposition and pulmonary inflammation after short-term inhalation of silver nanoparticles. Particle and Fibre Toxicology, 11, 49. 10.1186/s12989-014-0049-1 [PubMed: 25227272]

DeLoid G, Cohen JM, Darrah T, Derk R, Rojanasakul L, Pyrgiotakis G, & Demokritou P (2014). Estimating the effective density of engineered nanomaterials for in vitro dosimetry. Nature Communications, 5, 3514. 10.1038/ncomms4514

Fröhlich E (2018). Comparison of conventional and advanced in vitro models in the toxicity testing of nanoparticles. Artif Cells Nanomed Biotechnol, 46(2), 1091–1107. 10.1080/21691401.2018.1479709 [PubMed: 29956556]

Fröhlich E, Mercuri A, Wu S, & Salar-Behzadi S (2016). Measurements of deposition, lung surface area and lung fluid for simulation of inhaled compounds. Frontiers in Pharmacology, 7, 181. 10.3389/fphar.2016.00181 [PubMed: 27445817]

Grotber JB (2011). Respiratory fluid mechanics. Physics of Fluids, 23(2), Article 21301. 10.1063/1.3517737 [PubMed: 21403768]

Hendren CO, Mesnard X, Droge J, & Wiesner MR (2011). Estimating production data for five engineered nanomaterials as a basis for exposure assessment. Environmental Science and Technology, 45(7), 2562–2569. 10.1021/es103300g [PubMed: 21391627]

Hinderliter PM, Minard KR, Orr G, Chrisler WB, Thrall BD, Pounds JG, & Teeguarden JG (2010). Isdd: A computational model of particle sedimentation, diffusion and target cell dosimetry for in vitro toxicity studies. Particle and Fibre Toxicology, 7(1), 36. 10.1186/1743-8977-7-36 [PubMed: 21118529]

ICRP. (2002). Basic anatomical and physiological data for use in radiological protection reference values. ICRP publication 89. Annals of the ICRP, 32(3–4).

Johnston HJ, Hutchison G, Christensen FM, Peters S, Hankin S, & Stone V (2010). A review of the in vivo and in vitro toxicity of silver and gold particulates: Particle attributes and biological mechanisms responsible for the observed toxicity. Critical Reviews in Toxicology, 40(4), 328–346. 10.3109/10408440903453074 [PubMed: 20128631]

Jo MS, Kim JK, Kim Y, Kim HP, Kim HS, Ahn K, & Yu IJ (2020). Mode of silver clearance following 28-day inhalation exposure to silver nanoparticles determined from lung burden assessment including post-exposure observation periods. Archiv für Toxikologie, 94(3), 773–784. 10.1007/s00204-020-02660-2 [PubMed: 32157349]

Kabilan S, Suffield SR, Recknagle KP, Jacob RE, Einstein DR, Kuprat AP, & Corley RA (2016). Computational fluid dynamics modeling of Bacillus anthracis spore deposition in rabbit and human respiratory airways. Journal of Aerosol Science, 99, 64–77. 10.1016/j.jaerosci.2016.01.011 [PubMed: 33311732]

Kreyling WG, Holzwarth U, Hirn S, Schleh C, Wenk A, Schäffler M, & Gibson N (2020). Quantitative biokinetics over a 28 day period of freshly generated, pristine, 20 nm silver nanoparticle aerosols in healthy adult rats after a single 1½-hour inhalation exposure. Particle and Fibre Toxicology, 17(1), 21. 10.1186/s12989-020-00347-1 [PubMed: 32503677]

NIOSH. (2018). In Kuempel ED, Roberts JR, G. 20 Roth, Zumwalde RD, Drew N, Hubbs A, Dunn KL, Trout D, & Cincinnati HG (Eds.), Revised external review draft - current intelligence bulletin: Health 19 effects of occupational exposure to silver nanomaterials. 21 OH: U.S. Department of Health and Human Services, Centers for Disease Control and 22 Prevention, National Institute for Occupational Safety and Health.

Kumar V, Sharma N, & Maitra SS (2017). In vitro and in vivo toxicity assessment of nanoparticles. International Nano Letters, 7(4), 243–256. 10.1007/s40089-017-0221-3

Lee JH, Kwon M, Ji JH, Kang CS, Ahn KH, Han JH, & Yu IJ (2011). Exposure assessment of workplaces manufacturing nanosized TiO2 and silver. Inhalation Toxicology, 23(4), 226–236. 10.3109/08958378.2011.562567 [PubMed: 21456955]

Leo BF, Chen S, Kyo Y, Herpoldt K-L, Terrill NJ, Dunlop IE, & Ryan MP (2013). The stability of silver nanoparticles in a model of pulmonary surfactant. Environmental Science & Technology, 47(19), 11232–11240. 10.1021/es403377p [PubMed: 23988335]

Liu J, & Hurt RH (2010). Ion release kinetics and particle persistence in aqueous nano-silver colloids. Environmental Science and Technology, 44(6), 2169–2175. 10.1021/es9035557 [PubMed: 20175529]

Liu J, Sonshine DA, Shervani S, & Hurt RH (2010). Controlled release of biologically active silver from nanosilver surfaces. ACS Nano, 4(11), 6903–6913. 10.1021/nn102272n [PubMed: 20968290]

Liu J, Wang Z, Liu FD, Kane AB, & Hurt RH (2012). Chemical transformations of nanosilver in biological environments. ACS Nano, 6(11), 9887–9899. 10.1021/nn303449n [PubMed: 23046098]

Maurer EI, Sharma M, Schlager JJ, & Hussain SM (2014). Systematic analysis of silver nanoparticle ionic dissolution by tangential flow filtration: Toxicological implications. Nanotoxicology, 8(7), 718–727. 10.3109/17435390.2013.824127 [PubMed: 23848466]

Miller FJ, Asgharian B, Schroeter JD, & Price O (2016). Improvements and additions to the multiple path particle dosimetry model. Journal of Aerosol Science, 99, 14–26. 10.1016/j.jaerosci.2016.01.018

Munusamy P, Wang C, Engelhard MH, Baer DR, Smith JN, Liu C, & Ryan MP (2015). Comparison of 20 nm silver nanoparticles synthesized with and without a gold core: Structure, dissolution in cell culture media, and biological impact on macrophages. Biointerphases, 10(3), Article 31003. 10.1116/1.4926547

Nel A, Xia T, Meng H, Wang X, Lin S, Ji Z, & Zhang H (2013). Nanomaterial toxicity testing in the 21st Century: Use of a predictive toxicological approach and high-throughput screening. Accounts of Chemical Research, 46(3), 607–621. 10.1021/ar300022h [PubMed: 22676423]

Ng AW, Bidani A, & Heming TA (2004). Innate host defense of the lung: Effects of lung-lining fluid pH. Lung, 182(5), 297–317. 10.1007/s00408004-2511-6 [PubMed: 15742242]

Nowack B, Krug HF, & Height M (2011). 120 years of nanosilver history: Implications for policy makers. Environmental Science and Technology, 45(4), 1177–1183. 10.1021/es103316q [PubMed: 21218770]

Park JD, Kim JK, Jo MS, Kim YH, Jeon KS, Lee JH, & Yu IJ (2019). Lobar evenness of deposition/retention in rat lungs of inhaled silver nanoparticles: An approach for reducing animal use while maximizing endpoints. Particle and Fibre Toxicology, 16(1), Article 2–2. 10.1186/s12989-018-0286-9 [PubMed: 30616672]

Paur H-R, Cassee FR, Teeguarden J, Fissan H, Diabate S, Aufderheide M, & Schmid O (2011). In-vitro cell exposure studies for the assessment of nanoparticle toxicity in the lung—a dialog between aerosol science and biology. Journal of Aerosol Science, 42(10), 668–692. 10.1016/j.jaerosci.2011.06.005

Reidy B, Haase A, Luch A, Dawson KA, & Lynch I (2013). Mechanisms of silver nanoparticle release, transformation and toxicity: A critical review of current knowledge and recommendations for future studies and applications. Materials, 6(6), 2295–2350. 10.3390/ma6062295 [PubMed: 28809275]

Savage DT, Hilt JZ, & Dziubla TD (2019). In vitro methods for assessing nanoparticle toxicity. Methods in Molecular Biology, 1894, 1–29. 10.1007/978-1-4939-8916-4_1 [PubMed: 30547452]

Schmid O, & Cassee FR (2017). On the pivotal role of dose for particle toxicology and risk assessment: Exposure is a poor surrogate for delivered dose. Particle and Fibre Toxicology, 14(1), Article 52–52. 10.1186/s12989-017-0233-1 [PubMed: 29216928]

Sharma G, Kodali V, Gaffrey M, Wang W, Minard KR, Karin NJ, & Thrall BD (2014). Iron oxide nanoparticle agglomeration influences dose rates and modulates oxidative stress-mediated dose-response profiles in vitro. Nanotoxicology, 8(6), 663–675. 10.3109/17435390.2013.822115 [PubMed: 23837572]

Smith JN, Thomas DG, Jolley H, Kodali VK, Littke MH, Munusamy P, & Teeguarden JG (2018). All that is silver is not toxic: Silver ion and particle kinetics reveals the role of silver ion aging and dosimetry on the toxicity of silver nanoparticles. Particle and Fibre Toxicology, 15(1), 47. 10.1186/s12989-018-0283-z [PubMed: 30518385]

Stebounova LV, Guio E, & Grassian VH (2011). Silver nanoparticles in simulated biological media: A study of aggregation, sedimentation, and dissolution. Journal of Nanoparticle Research, 13(1), 233–244. 10.1007/s11051-010-0022-3

Stephens RH, Benjamin AR, & Walters DV (1996). Volume and protein concentration of epithelial lining liquid in perfused in situ postnatal sheep lungs. Journal of Applied Physiology, 80(6), 1911–1920. 10.1152/jappl.1996.80.6.1911 [PubMed: 8806894]

Sweeney S, Leo BF, Chen S, Abraham-Thomas N, Thorley AJ, Gow A, & Tetley TD (2016). Pulmonary surfactant mitigates silver nanoparticle toxicity in human alveolar type-I-like epithelial cells. Colloids and Surfaces B: Biointerfaces, 145, 167–175. 10.1016/j.colsurfb.2016.04.040 [PubMed: 27182651]

Teeguarden JG, Hinderliter PM, Orr G, Thrall BD, & Pounds JG (2007). Particokinetics in vitro: Dosimetry considerations for in vitro nanoparticle toxicity assessments. Toxicological Sciences, 95(2), 300–312. 10.1093/toxsci/kfl165 [PubMed: 17098817]

Teeguarden JG, Mikheev VB, Minard KR, Forsythe WC, Wang W, Sharma G, & Thrall BD (2014). Comparative iron oxide nanoparticle cellular dosimetry and response in mice by the inhalation and liquid cell culture exposure routes. Particle and Fibre Toxicology, 11, 46. 10.1186/s12989-014-0046-4 [PubMed: 25266609]

Thomas DG, Smith JN, Thrall BD, Baer DR, Jolley H, Munusamy P, & Teeguarden JG (2018). ISD3: A particokinetic model for predicting the combined effects of particle sedimentation, diffusion and dissolution on cellular dosimetry for in vitro systems. Particle and Fibre Toxicology, 15(1), 6. 10.1186/s12989-018-0243-7 [PubMed: 29368623]

Wauthoz N, & Amighi K (2015). Formulation strategies for pulmonary delivery of poorly soluble drugs. In Nokhodchi A, & Martin GP (Eds.), Pulmonary drug delivery (pp. 87–122).

Weldon BA, Faustman EM, Oberdörster G, Workman T, Griffith WC, Kneuer C, & Yu IJ (2016). Occupational exposure limit for silver nanoparticles: Considerations on the derivation of a general health-based value. Nanotoxicology, 10(7), 945–956. 10.3109/17435390.2016.1148793 [PubMed: 26982810]

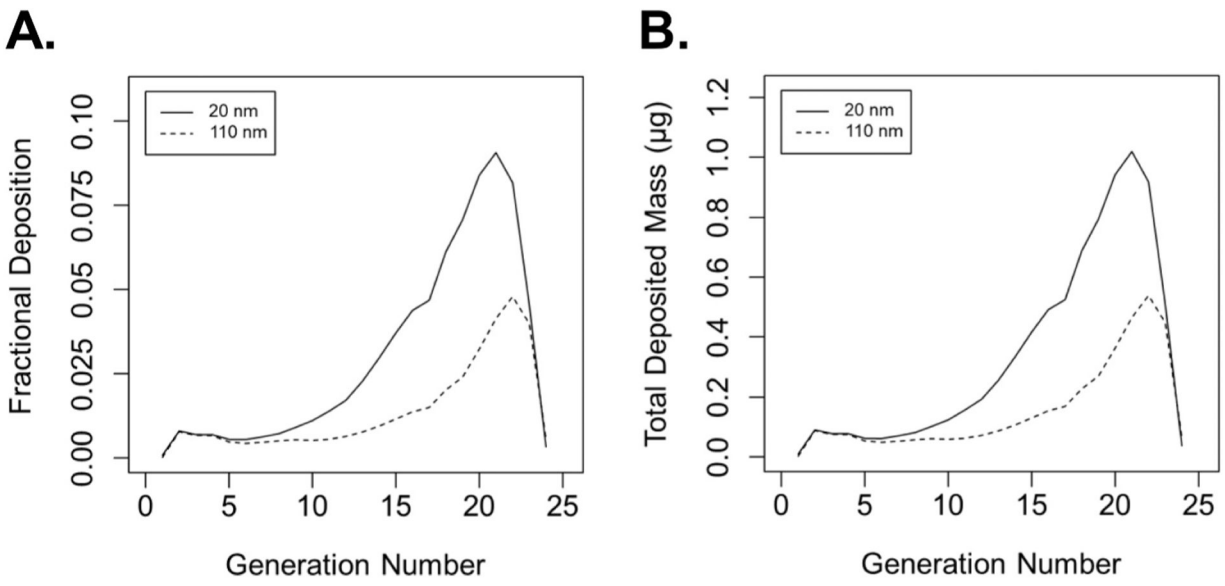

Fig. 1.

Multiple-Path Particle Dosimetry (MPPD) Model simulated fractional deposition (**A**) and total mass deposited (**B**) of silver nanoparticles as a function of pulmonary generation number in humans exposed to 20 or 110 nm at 0.9 μg/m^3 for 8 h.

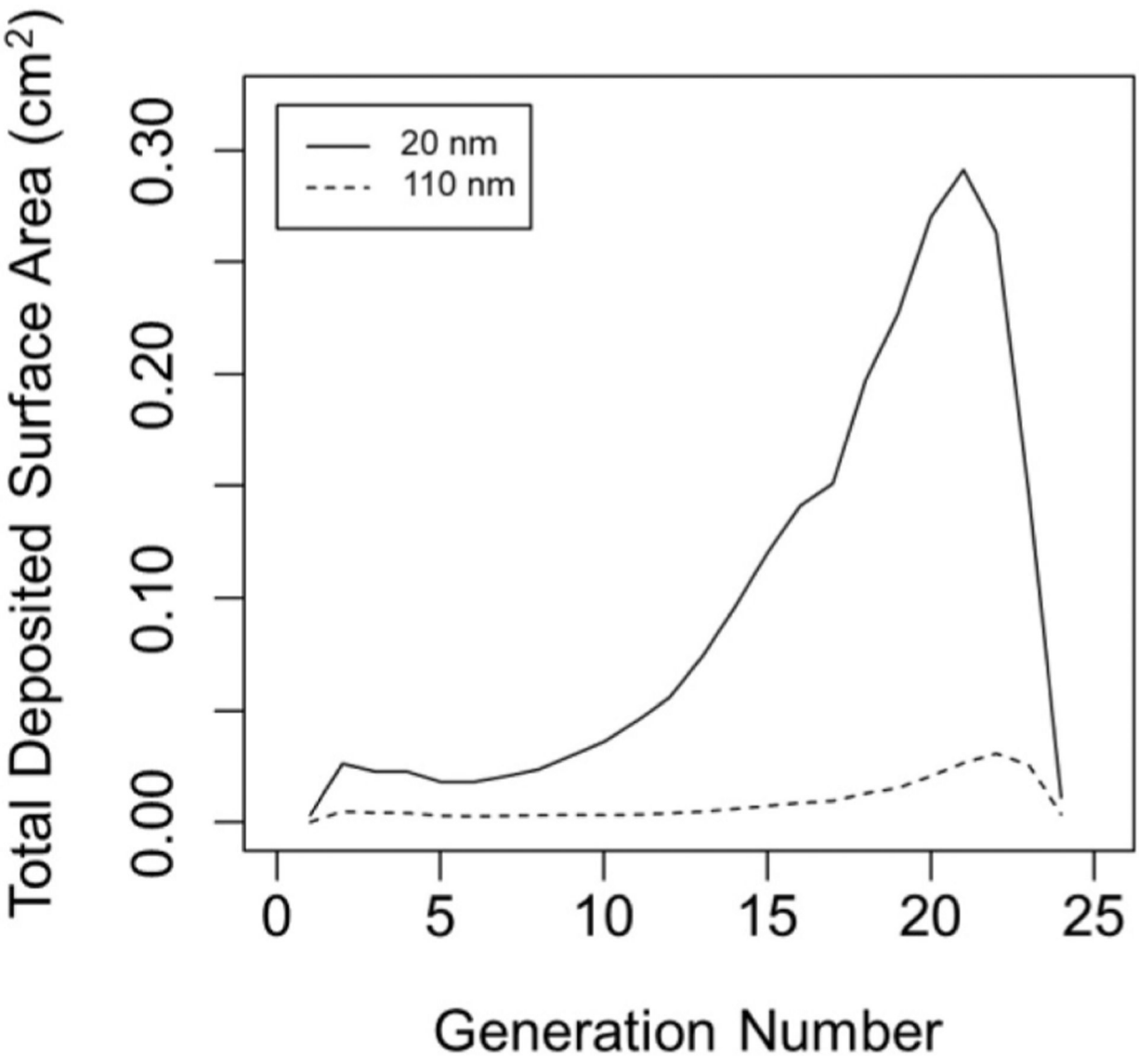

Fig. 2.

Multiple-Path Particle Dosimetry (MPPD) Model simulated total nanoparticle surface area deposited as a function of pulmonary generation number in humans exposed to 20 or 110 nm silver nanoparticles at 0.9 μg/m^3 for 8 h.

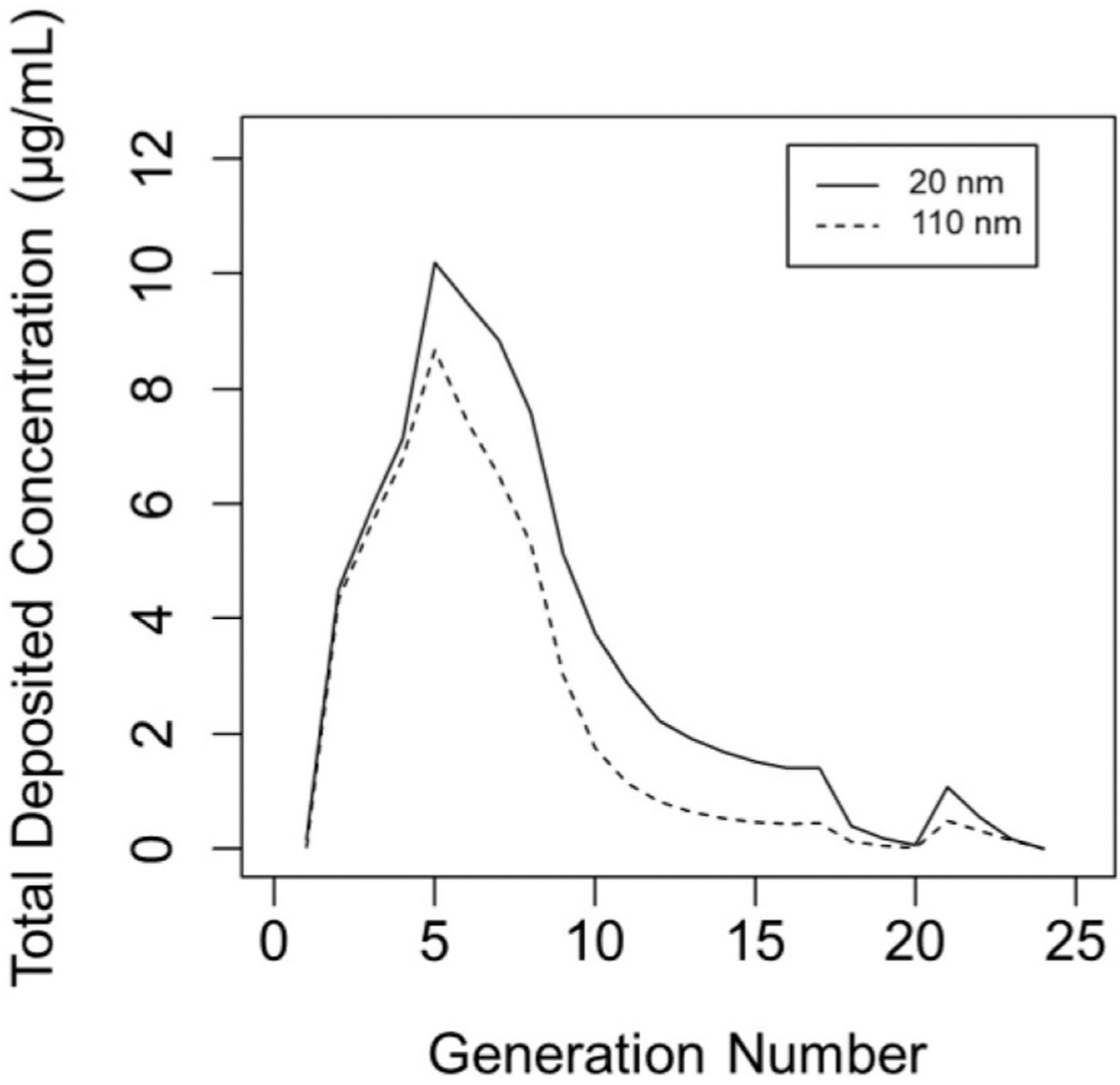

Fig. 3.

Multiple-Path Particle Dosimetry (MPPD) Model simulated total deposited nanoparticle concentration as a function of pulmonary generation number in humans exposed to 20 or 110 nm silver nanoparticles at 0.9 µg/m^3 for 8 h.

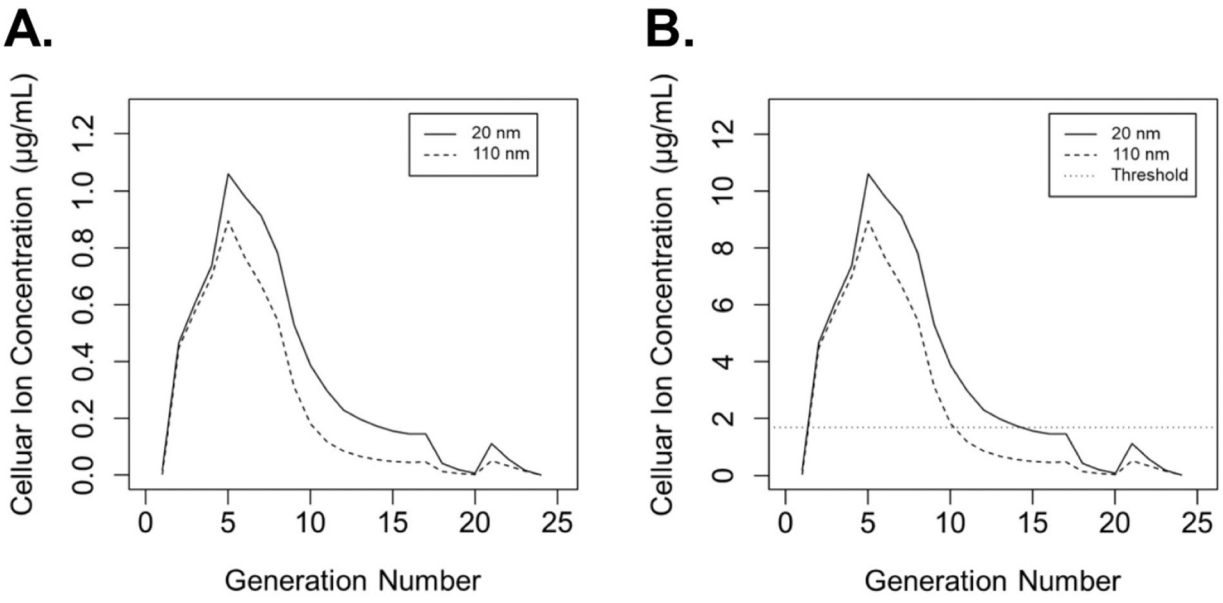

Fig. 4.

Predicted silver ion concentrations in tissues resulting from humans exposed to 20 or 110 nm silver nanoparticles at 0.9 µg/m^3 for 8 h, assuming 0.4 (**A**) and 4% (**B**) nanoparticle dissolution by mass. The dotted line represents a toxic threshold concentration of silver ions in cells causing 20% loss of viability in macrophages (Smith et al., 2018).

Table 1

Nanoparticle parameters used to simulate human exposures to silver nanoparticles using the Multiple-Path Particle Dosimetry (MPPD) Model.

Parameter	Particle	
Diameter (nm)	20	110
Density (g/cm^3)	10.49	10.49
Geometric Standard Deviation (GSD)	1	1
Aerosol Concentration (μg/m^3)	0.9	0.9
Aspect Ratio	1	1
Surface area (cm^2/mg)	286	52

Table 2

Pulmonary physiological parameters used to simulate human exposures to silver nanoparticles using the Multiple-Path Particle Dosimetry (MPPD) Model.

Parameter	Value
Functional residual capacity (FRC)	3300 mL
Upper respiratory tract volume (URT)	50 mL
Tidal volume	1300 mL
Breathing rate	20 breaths/min
Inspiratory fraction	0.5
Pause fraction	0
Breathing Scenario	Oronasal-Mouth Augmenter

Table 3

Pulmonary surface area, lung lining fluid depth, and lung lining fluid volumes used to simulate human exposures to silver nanoparticles using the Multiple-Path Particle Dosimetry (MPPD) Model.

Generation Number	Structure	Pulmonary surface area (cm^2)	Lung lining fluid depth (μm)[a]	Lung lining fluid volume (mL)
1	Trachea	29	20	0.06
2	Main bronchus	25	8	0.02
3	Second bronchus	17	8	0.01
4	Segment bronchus	14	8	0.01
5	Bronchi(ole)	18	3.5	0.01
6	Bronchi(ole)	19	3.5	0.01
7	Bronchi(ole)	23	3.5	0.01
8	Bronchi(ole)	31	3.5	0.01
9	Bronchi(ole)	58	3.5	0.02
10	Bronchi(ole)	96	3.5	0.03
11	Bronchi(ole)	156	3.5	0.05
12	Bronchi(ole)	248	3.5	0.09
13	Bronchi(ole)	383	3.5	0.13
14	Bronchi(ole)	566	3.5	0.20
15	Bronchi(ole)	788	3.5	0.28
16	Bronchi(ole)	998	3.5	0.35
17	Bronchi(ole)	1063	3.5	0.37
18	Bronchi(ole)	4883	3.5	1.71
19	Respiratory bronchiole	12,250	3.5	4.29
20	Respiratory bronchiole	38,900	3.5	13.62
21	Proximal alveolar region	62,710	0.15	0.94
22	Distal alveolar region	110,100	0.15	1.65
23	Distal alveolar region	196,400	0.15	2.95
24	Distal alveolar region	361,800	0.15	5.43
Total		791,574		32.24

[a](Wauthoz & Amighi, 2015).